

## Using nonharmonic forcing to switch the periodicity in nonlinear systems

Miguel A. F. Sanjuán

*Escuela Superior de Ciencias Experimentales y Tecnología, Universidad Rey Juan Carlos, Camino de Humanes 63, 28936 Móstoles, Madrid, Spain*

(Received 8 July 1997; revised manuscript received 1 June 1998)

Once the parameters of a dynamical system are fixed, specific patterns of stable equilibrium, periodicity, quasiperiodicity, or chaos are obtained. Keeping the same parameters and simply modifying the wave form and periodicity of the driving force allows switching from one orbit to another. In this way the options to select a more desirable periodic orbit are increased. This is particularly important in some systems where changing the internal parameters of the system is not possible or at least very inconvenient. [S1063-651X(98)08209-9]

PACS number(s): 05.45.+b

### I. INTRODUCTION

Many physical phenomena are modeled by periodically driven dynamical systems. They may appear in fields such as lasers [1,2], mechanical engineering [3], superconductor junctions [4], etc., which illustrates the broad applicability of studying these systems. In the following we assume we have a periodically driven dynamical system. Think of a one-dimensional, damped and nonautonomous nonlinear oscillator for definiteness. The general equation of motion, with dissipation and external periodic forcing, may be written as

$$\ddot{x} + \delta\dot{x} + dV/dx = f(t), \quad (1)$$

where we may assume the driving force to be the harmonic function  $f(t) = \gamma \cos \omega t$  of period  $T = 2\pi/\omega$ . The variable  $x(t)$  is the position at time  $t$  and  $\delta$  is the damping coefficient. The parameters  $\gamma$  and  $\omega$  are the amplitude and frequency of the perturbation. The potential of the restoring force is  $V(x)$ .

The system depends on several parameters that determine the asymptotic dynamical states. Once all the parameters are fixed the solutions are uniquely determined. In general the possibilities are stable equilibrium states, periodic, quasiperiodic, and chaotic solutions. Generally, harmonic functions are used to excite dynamical systems either externally or parametrically. Moreover harmonic or trigonometric functions are the simplest solutions of the linear harmonic oscillator and are commonly used to drive linear oscillators. Even though they are not in general solutions of more complicated nonlinear dynamical systems, they are extensively used as general drivers of nonlinear oscillators, as well. In the case of a nonlinear oscillator things are known to be more complex. In simple nonlinear oscillators such as the pendulum or the Duffing oscillator the solutions are Jacobi elliptic functions, and hence it seems natural to use these functions as drivers, instead of a harmonic function.

One of the main questions we address here is the investigation of the effect on the dynamics of using Jacobi elliptic functions as drivers, while the rest of the parameters of the system are kept fixed. In particular we want to show how in these circumstances, its use allows new accessible states.

To clarify this idea, we could think of driving the system with a more general periodic function  $f(t, m) = f(t + T, m)$  of period  $T$ , with an ‘‘extra’’ parameter  $m$ . Let us assume that

this parameter changes continuously in  $0 \leq m \leq 1$ . To be faithful to the original system,  $f(t, m)$  should be such that  $m = 0$  coincides with the original driving. If this were possible, using the same set of parameters for  $m = 0$ , we could still have a new degree of freedom  $m$ .

One family of functions that possesses this property are the *Jacobi elliptic functions*. These are precisely the natural solutions to many nonlinear oscillators, such as those with a polynomial restoring force, like Duffing oscillators and variations including quadratic nonlinearities, and the nonlinear pendulum. The main advantage to using them as drivers of dynamical systems lies in the very nature of these functions and consequently they have been already used by some authors [5–7]. So, the fact of using them as drivers is not capricious, as it could be perceived by the reader who is very much used to seeing trigonometric functions to drive systems. There are simple and deep reasons for doing it. They are periodic functions whose period and wave form depend on  $m$ . Furthermore, it has an increasing number of modes as  $m$  increases, and its Fourier spectrum is more complicated than the usual trigonometric functions.

The main goal of this paper is to show, with the example of a nonlinear pendulum parametrically forced with a Jacobi elliptic function, that we can switch the periodicity of a solution by simply changing the wave form and periodicity of the driving force, but without changing the rest of the parameters. Transitions from chaotic states into periodic states by periodic driving has been previously demonstrated [5–7], but here in addition we have transitions among periodic states. Another point of interest of this paper is to throw light on a better understanding of this kind of driving. In cases in which changing other parameters of the system could be difficult or impossible, this gives an alternative way of modifying the periodicity of the solutions of the system. We show also this possibility by comparing the result of using a trigonometric function and a Jacobi elliptic function of equivalent amplitude and period, in such a way that only the wave form of the driver permits these periodic transitions. The paper is organized as follows: Sec. II reports on some characteristics of Jacobi elliptic functions. With them, we perturb a pendulum parametrically and the model is described in Sec. III. The model depends on a series of parameters, and the asymptotic dynamical properties of the system are analyzed with the help of the chaotic parameter set, which is con-

structed by varying two parameters simultaneously and to which is devoted Sec. IV. To show further evidence of the effect of using nonharmonic driving to switch the periodicity, we compare the effect of using two different drivers with equal amplitude and period, but different wave form in Sec. V. Finally, Sec. VI includes a summary of results and conclusions.

## II. JACOBI ELLIPTIC FUNCTIONS

The parametric perturbation we consider is the cosine amplitude Jacobi elliptic function  $\text{cn}(\omega t, m)$  of frequency  $\omega$  and elliptic parameter  $m$  [8], and its use has the advantage of providing a new degree of freedom in the parameter space. Furthermore, it has a more sophisticated Fourier spectrum than the trigonometric functions and the exact analytical solutions of the pendulum without forcing term are of this type.

The most common Jacobi elliptic functions are  $\text{cn}(\omega t, m)$  and  $\text{sn}(\omega t, m)$ ,  $0 \leq m \leq 1$ , and they are periodic functions of period  $T = 4K(m)/\omega$ , where  $K(m)$  is the *complete elliptic integral of the first kind* [10,11] and is defined as

$$K(m) = \int_0^{\pi/2} \frac{d\vartheta}{\sqrt{1 - m \sin^2 \vartheta}}. \quad (2)$$

There are two natural limits for these functions: the *trigonometric limit*,  $m=0$ , which gives  $\cos \omega t$  and  $\sin \omega t$ , respectively, and the *hyperbolic limit*,  $m=1$ , which gives  $\text{sech } \omega t$  and  $\tanh \omega t$ , respectively [9].

A physical and intuitive picture of the meaning of  $m$  may be obtained by thinking of the unperturbed orbits in phase space inside a separatrix orbit. The parameter  $m$  is used to label the energy of the orbits inside the separatrix. For orbits with energy very small in absolute terms, i.e.,  $m \rightarrow 0$ , the complete elliptic integral of the first kind  $K(m) \rightarrow \pi/2$  and then the period becomes  $T \rightarrow 2\pi$ . This is obviously the period for the linear oscillations around the elliptic fixed point. However, for values of the energy close to the separatrix, which means  $m \rightarrow 1$ , the complete elliptic integral of the first kind diverges logarithmically [10,11] and the period becomes infinity.

Figure 1 provides a more clear idea of the nature of the driving we are using, showing the dependence versus time of  $\text{cn}(t, m)$  for some values of  $m$ . The periodic function  $f(t)$  of period  $T$  that is used as a driver in Eq. (1) could be written as  $f(t) = \gamma \text{cn}(\Omega t; m)$ , whose frequency varies with  $m$  and is given by  $\Omega(m) = 4K(m)/T$ . Assuming we keep  $T$  constant and equal to  $2\pi/\omega$ , ( $\omega > 0$ , a constant), this implies that the functions  $f(t) = \gamma \text{cn}(2\omega K(m)t/\pi; m)$  and  $g(t) = \gamma \cos(\omega t)$  have equal period and amplitude and they only differ on the parameter  $m$ .

## III. PARAMETRIC PENDULUM

The physical system under consideration is a pendulum moving in a plane whose pivot is subjected to a nonharmonic vertical periodic displacement  $\text{cn}(\omega t, m)$  of amplitude  $\gamma$  and frequency  $\omega$ ; see Fig. 2. The equation of motion reads

$$\ddot{\theta} + \delta \dot{\theta} + [1 + \gamma \text{cn}(\omega t, m)] \sin \theta = 0, \quad (3)$$

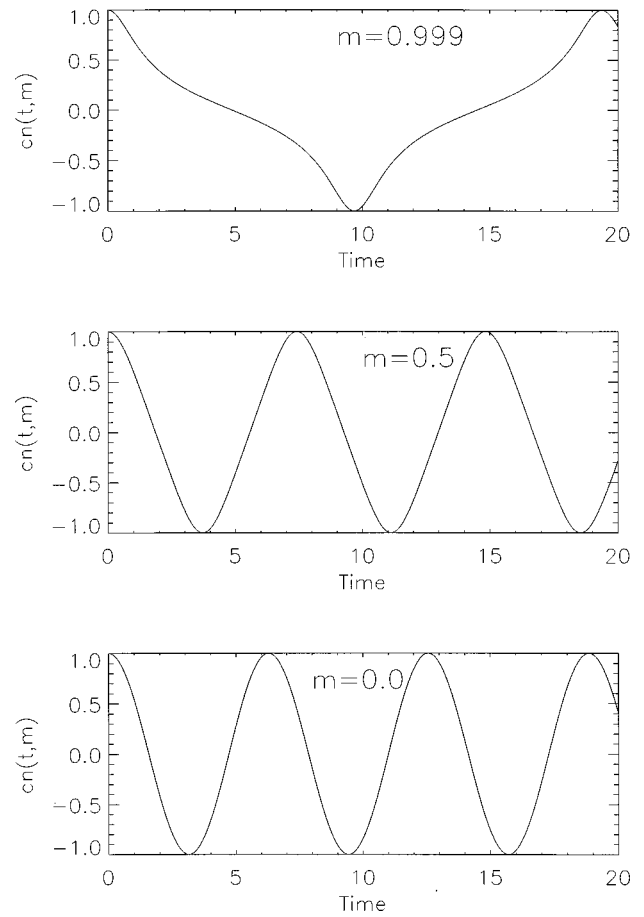


FIG. 1. The variations of the  $\text{cn}(t, m)$  vs time for some values of  $m$  are shown. Observe the change of the wave form and the period of the wave.

where  $-\pi \leq \theta \leq \pi$  represents the angle of displacement and  $\delta$  the damping coefficient. The trigonometric limit,  $m=0$ , has been studied previously numerically [12,13], analytically [14], and experimentally [15] by several authors. Analytical results showing estimations of the homoclinic bifurcations and subharmonic bifurcations, using Melnikov's theory, for the nonharmonic perturbation of the parametric pendulum are found in [16].

In spite of its simplicity, this system is known to have for  $m=0$  a rich variety of dynamical solutions including stable equilibria, periodic oscillations, rotations, and chaotic solutions, depending strongly on the parameters of the system  $\gamma, \omega, \delta$  and the initial conditions, that is,  $\theta(t_0)$  and  $\dot{\theta}(t_0)$ . The oscillations around the position  $\theta=0$  are bounded in the region  $-\pi \leq \theta \leq \pi$ . Rotations, however, are unbounded, going above  $\theta = \pm \pi$ . When  $\dot{\theta}(t) > 0$  they are clockwise and when  $\dot{\theta}(t) < 0$  they are anticlockwise. More information about the parametrically forced pendulum using a trigonometric function as driver can be found in [17].

## IV. CHAOTIC PARAMETRIC SET

For the numerical computations and for convenience  $\delta = 0.1$  and  $\omega = 1.5$  are set, hence only the parameters  $\gamma$  and  $m$  are free. Fixing  $m=0$  means that a circular function is used to perturb the system and consequently only one parameter is

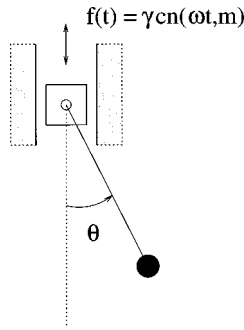


FIG. 2. Simple pendulum with a nonharmonic vertical oscillating support given by the cosine amplitude elliptic function.

free. In the general case we can study the chaotic parametric set by varying the two parameters simultaneously. Figure 3 shows the *chaotic parametric set* for the parameters  $\gamma$  and  $m$  of Eq. (3) and it is constructed as follows. Take a grid of  $240 \times 200$  points in the rectangle of parameter values  $-5 < \gamma < 5$  and  $1 < m < 0$ . For each pair of parameters  $(\gamma, m)$  in the parameter plane the differential equation is solved by using a fourth order Runge-Kutta integrator, using  $[\theta(t_0), \dot{\theta}(t_0)] = (1, 0)$  as initial condition. The Lyapunov exponent of the corresponding orbit is evaluated by standard methods and then a different color is assigned depending on the sign of the Lyapunov exponent. Those points in the  $(\gamma, m)$  plane with a negative Lyapunov exponent are marked white, while those with a positive Lyapunov exponent are black. As the reader may imagine, this process is heavily time consuming. The resulting plot displays global information about the parameter regions with periodic or nonperiodic behavior.

From Fig. 3, it can be inferred that there is a “periodic sea” and there are “chaotic islands” similar to the ones described in [6,7] for the single-well Duffing oscillator. “Periodic lakes” and “periodic channels” in some of the chaotic islands are also observed. Notice the striations in some of the islands; these are windows of periodicity inside the chaotic islands. Similar windows have been described and analyzed very recently in the context of higher-dimensional

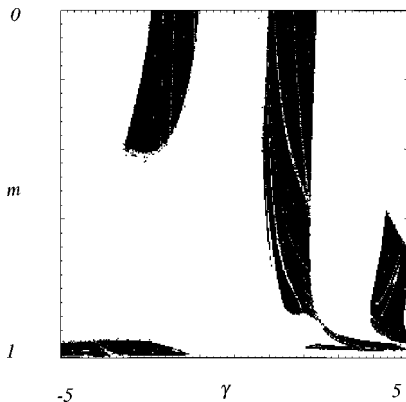


FIG. 3. Chaotic parameter set for the two parameters  $\gamma$  and  $m$ . The vertical variable is  $1 < m < 0$  while the horizontal one is  $-5 < \gamma < 5$ . Those points with a negative Lyapunov exponent are marked white, while those with a positive Lyapunov exponent are black. The upper line corresponds to  $m = 0$  and  $-5 < \gamma < 5$ , showing a kind of bifurcation diagram.

chaotic systems by Barreto *et al.* [18] and they conjecture that these kinds of windows should appear commonly in dynamical systems.

Each horizontal line crossing the figure may be also understood as a kind of bifurcation diagram. In particular if we draw a horizontal line by  $m = 0.2$  and we vary  $\gamma$  from  $-5$  to  $5$ , we see that there are two chaotic regions corresponding to the black dots traversed by this line. On the other hand, we may draw a vertical line at a certain fixed value of  $\gamma$  and vary  $m$  from  $0$  to  $1$ . In particular and as we will see later, drawing a vertical line at  $\gamma = -4$  we see that this line crosses the black region only in a small range of values of  $m$  close to  $m = 1$ . Fixing the attention on this last vertical line at  $\gamma = -4$ , we realize that for most values of  $m$  the Lyapunov exponents are negative, however, many different periodic orbits “live” through this line.

The boundaries of the chaotic islands are basically smooth. From an “island,” with a positive Lyapunov exponent, we can go to the “sea” by modifying either the amplitude of the perturbation  $\gamma$  or the elliptic parameter  $m$ . Numerical evidence shows that most transitions from a chaotic island to the periodic sea are via saddle-node bifurcations. Period-doubling bifurcations are observed, however, in transitions between the “channels.” The “lakes” contain periodic orbits, in particular the small lake in the bottom left island is a period-4 lake.

Note that in the region of parameters  $(\gamma, m)$  considered in Fig. 3, once a value of  $\gamma$  is fixed, we can always find a periodic solution by simply selecting the appropriate elliptic parameter  $m$ .

Next, we consider some examples of orbits for the parametrically excited pendulum with all the parameters fixed. Only the elliptic parameter  $m$  is modified, allowing the character of the solution to be changed. In Fig. 4 periodic orbits for some values of  $m$  are shown. Due to the symmetry of the system every orbit has a symmetric counterpart with the symmetry  $\theta \rightarrow -\theta$  and  $\dot{\theta} \rightarrow -\dot{\theta}$ . For some values of  $m$  we have found up to five different coexisting periodic attractors.

In Fig. 5 some periodic oscillations of different periods for distinct values of  $m$  are shown. Also a chaotic strange attractor that exists for a very narrow parameter region between  $0.9 \leq m \leq 0.999$  is shown. This means that once all the parameters are set, one can still change the dynamics of the system with the nonharmonic perturbation.

Extensive numerical computations give evidence of this phenomenon and how by simply changing  $m$  we can switch from one periodic state to another one. In fact the multiplicity of coexisting attractors inside the periodic sea is considerable, presenting a very rich variety of periodic states.

It should be stressed, however, that even though for certain parameter values many periodic attractors may coexist, the basins of attraction of most of them are very small and difficult to detect unless a fine resolution is used. This implies that selecting a specific stable periodic orbit is experimentally very difficult because noise would tend to push the trajectory away from these small basins. Moreover, coexisting attractors appear in a narrow zone in parameter space.

### V. USING DRIVERS OF EQUAL PERIOD AND AMPLITUDE, BUT DIFFERENT WAVE FORM

As observed in Fig. 1, the period of the Jacobi elliptic function varies continuously with  $m$ . Consequently a forcing

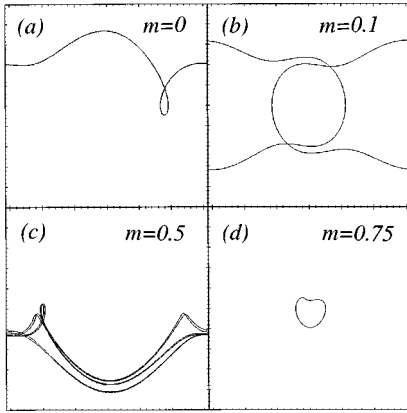


FIG. 4. Phase-space portraits of four different periodic orbits for  $\gamma = -4$  and different values of the elliptic parameter  $m$  are shown. The horizontal scale is  $-\pi \leq \theta \leq \pi$ , while the vertical scale is  $-5 \leq \dot{\theta} \leq 5$ . (a) Period-1 rotation for  $m=0$ . (b) Period 2 for  $m=0.1$ . (c) Period-6 rotation for  $m=0.5$ . (d) Period-1 oscillation for  $m=0.75$ .

of equal period and amplitude as the cosine function could be considered. Then it is possible to compare the effects on the dynamics of the parametric pendulum with the use of the harmonic function versus the nonharmonic function as forcings. This provides further evidence of the effect of the wave form in making possible transitions among periodic states, since the rest of the parameters are all equal.

The period of the cosine function is  $T = 2\pi/\omega$  and the period of the cn function is  $T = 4K(m)/\Omega(m)$ . If both functions are of equal period, this implies that  $\Omega(m) = 2\omega K(m)/\pi$ .

We can compare the effects of using as drivers two different perturbations  $\cos \omega t$  and  $\text{cn}[\Omega(m)t; m]$  with equal period and equal amplitude. In this case the only real difference between both perturbations is the elliptic parameter  $m$ , which accounts for the shape of the wave. The functions, both of them of period  $T = 2\pi/\omega$  ( $\omega = 1.5$ ), used to drive the parametric pendulum are shown in Fig. 6. The cosine function corresponds to  $m=0$  and the selected Jacobi elliptic

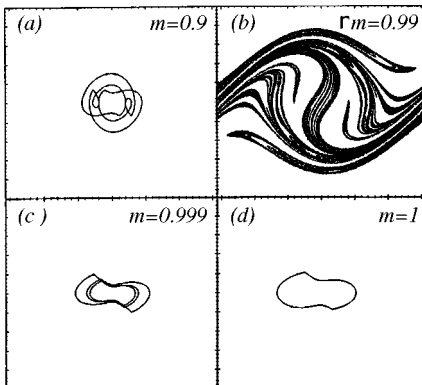


FIG. 5. The figure shows phase-space portraits of four different periodic orbits for  $\gamma = -4$  and different values of the elliptic parameter  $m$ . The horizontal scale is  $-\pi \leq \theta \leq \pi$ , while the vertical scale is  $-5 \leq \dot{\theta} \leq 5$ . (a) Period-4 oscillation for  $m=0.9$ . (b) Strange attractor for  $m=0.99$ . (c) Period-6 oscillation for  $m=0.999$ . (d) Period-2 oscillation for  $m=1$ .

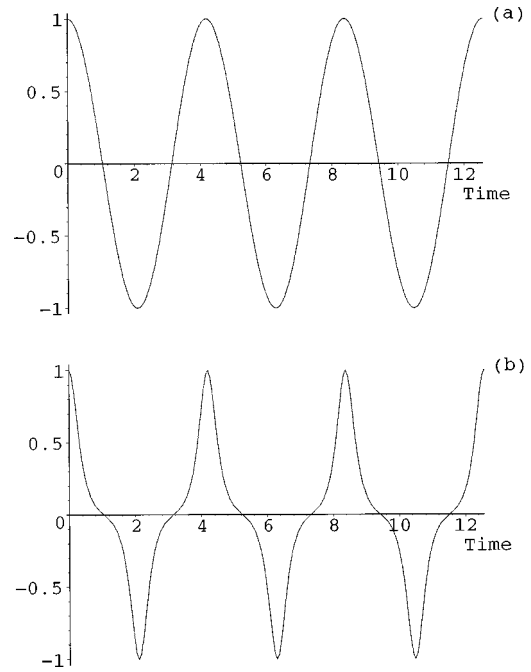


FIG. 6. Plot of the drivers, with equal amplitude and period, used to perturb the parametric pendulum, vs time. (a)  $\cos(1.5)t$  and (b)  $\text{cn}[(3/\pi)K(m)t; m]$  ( $m=0.999$ ).

function corresponds to  $m=0.999$ . Next, we introduce these functions in Eq. (3) and integrate the differential equations using a fourth order Runge-Kutta integrator, with initial conditions  $[\theta(t_0), \dot{\theta}(t_0)] = (1, 0)$ .

Using standard methods, we calculate the Lyapunov exponents with respect to the amplitude of the forcing for the two cases mentioned before, and for the values of the amplitude comprised between  $0 \leq \gamma \leq 5$ , and they are depicted in Fig. 7.

From the figure it can be observed that the regions corresponding to positive Lyapunov exponents are different, the case where the Jacobi elliptic function is used being a little more complicated. It could be thought that no difference would exist in the common parameter regions of negative Lyapunov exponents, that is, of periodic states. However, this is not the case, and what is verified is that the accessible states do not have the same periodicity. As a matter of fact, once all the parameters are fixed, we may compare the outputs for the same particular value of the amplitude and they correspond to periodic states of different periodicity for the same initial condition  $(1, 0)$ . Table I shows the variety of possible states available for different values of the amplitude  $\gamma$ , for the cosine driver ( $m=0$ ) and for the Jacobi elliptic function ( $m=0.999$ ). For a given initial condition, the possible transitions among periodic states are evidenced for a given amplitude by simply using a Jacobi elliptic function with the appropriate parameter  $m$ . Similarly to the case with  $m=0$ , many attractors of different periodicity coexist when  $m=0.999$  for a given value of the amplitude.

## VI. CONCLUSIONS

This work uses the parametric pendulum example to demonstrate the possibility of using nonharmonic perturbations

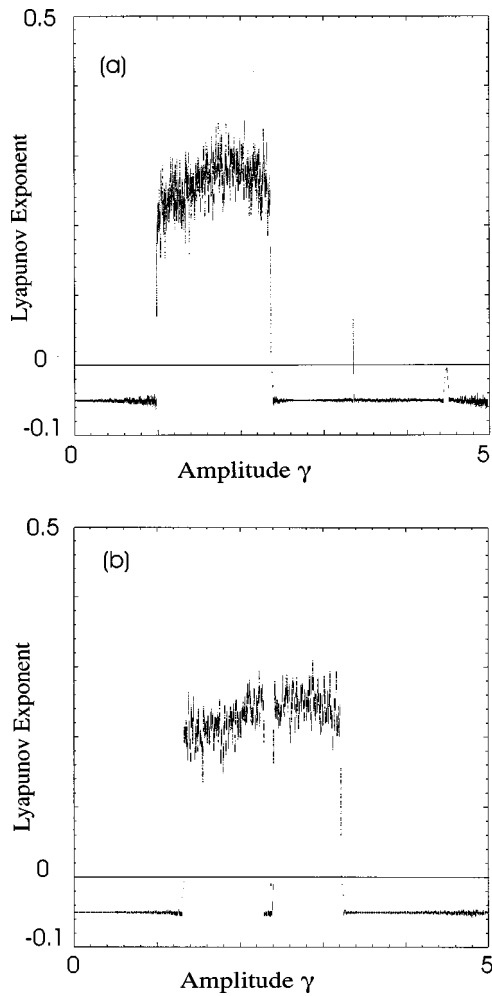


FIG. 7. Evolution of the Lyapunov exponents with respect to the variation of the amplitude of the driver  $\gamma$  in the interval  $0 \leq \gamma \leq 5$ . (a) When the function  $\cos(1.5)t$  is used as a driver, and (b) when the function  $\text{cn}[(3/\pi)K(m)t; m]$  ( $m=0.999$ ) is used.

to switch from one dynamic state to another without modifying the internal parameters of a system. This could conceivably allow shifting from one periodic orbit to another or

TABLE I. The solutions of the parametrically forced pendulum, for the initial condition  $(1,0)$  and for several values of the amplitude  $\gamma$ ,  $0 \leq \gamma \leq 5$ , are shown. The first column ( $m=0$ ) shows the solutions when the cosine function is used as driver and the second column ( $m=0.999$ ) shows the solutions when a cn Jacobi elliptic function of equal period is used. Note that for most cases the use of the nonharmonic driver implies a switch of periodicity.  $Pn$  means a periodic orbit of period  $n$ .

$\gamma$	$m=0$	$m=0.999$
0.65	$P2$	$P1$
1.2	chaos	$P1$
2	chaos <sup>a</sup>	chaos <sup>b</sup>
0.7	$P4$	$P1$
0.8	$P1$	$P2$
2.5	$P1$	chaos
3	$P1$	chaos
4	$P2$	$P1$
4.5	$P2$	$P1$
5	$P2$	$P1$

<sup>a</sup>Maximal Lyapunov exponent=1.329.

<sup>b</sup>Maximal Lyapunov exponent=1.276.

from a periodic to a chaotic trajectory. Further evidence of this fact is shown when two different functions of equal period and amplitude, but of different shape, are used. Such an approach may be useful in experimental situations (such as modulated lasers [7]) in which it is hard to modify system parameters.

#### ACKNOWLEDGMENTS

All of the computations have been made using the software DYNAMICS [19] and the codes used to compute the Jacobi elliptic functions were obtained from [20]. The author acknowledges fruitful comments and discussions with Ernest Barreto, Parvez Guzdar, Brian Hunt, and James A. Yorke. This work has been financed by DGICYT (Spain) under Project No. PR95-091 and by DGES (Spain) under Project No. PB96-0123.

- [1] K. S. Thornburg, Jr., M. Möller, R. Roy, T. W. Carr, R.-D. Li, and T. Erneux, *Phys. Rev. E* **55**, 3865 (1997).
- [2] I. B. Schwartz and I. Triandaf, *Phys. Rev. Lett.* **77**, 4740 (1996).
- [3] A. Venkatesan and M. Lakshmanan, *Phys. Rev. E* **55**, 5134 (1997).
- [4] G. Cicogna and L. Fronzoni, *Phys. Rev. A* **42**, 1901 (1990).
- [5] R. Chacón and J. Díaz Bejarano, *Phys. Rev. Lett.* **71**, 3103 (1993); R. Chacón, *Phys. Rev. E* **54**, 6153 (1996).
- [6] A. R. Zeni and J. A. C. Gallas, *Physica D* **89**, 71 (1995).
- [7] J. A. C. Gallas, *Appl. Phys. B: Photophys. Lasers Opt.* **60**, S203 (1995).
- [8] Notice that sometimes the *elliptic modulus*  $k$  is used instead where  $k^2=m$ .
- [9] It is interesting to note that there exists a model of plane ge-

- ometries, the nine plane Cayley-Klein geometries, where certain relationship between elliptic, Euclidean, and hyperbolic geometries is established [M. A. F. Sanjuán, *Int. J. Theor. Phys.* **23**, 1 (1984)], which recalls the one that appears here between the trigonometric, the hyperbolic, and the Jacobi elliptic functions.
- [10] D. Lawden, *Elliptic Functions and Applications* (Springer-Verlag, Berlin, 1989).
- [11] L. M. Milne-Thomson, in *Handbook of Mathematical Functions*, edited by M. Abramowitz and I. Stegun (Dover, New York, 1970).
- [12] J. B. McLaughlin, *J. Stat. Phys.* **24**, 375 (1981).
- [13] M. J. Clifford and S. R. Bishop, *Phys. Lett. A* **201**, 191 (1995).
- [14] B. P. Koch and R. W. Leven, *Physica D* **16**, 1 (1985).

- [15] J. Starret and R. Tagg, *Phys. Rev. Lett.* **74**, 1974 (1995).
- [16] M. A. F. Sanjuán, *Chaos Solitons Fractals* **7**, 435 (1996); **9**, 995 (1998).
- [17] S. R. Bishop, D. L. Xu, and M. J. Clifford, *Proc. R. Soc. London, Ser. A* **452**, 1789 (1996); S. R. Bishop and M. J. Clifford, *J. Sound Vib.* **189**, 142 (1996); R. Van Dooren, *ibid.* **200**, 105 (1997); D. Acheson, *From Calculus to Chaos* (Oxford University Press, Oxford, 1998), Chap. 12.
- [18] E. Barreto, B. R. Hunt, C. Grebogi, and J. A. Yorke, *Phys. Rev. Lett.* **78**, 4561 (1997).
- [19] H. E. Nusse and J. A. Yorke, *Dynamics: Numerical Explorations*, 2nd ed. (Springer-Verlag, New York, 1998).
- [20] W. H. Press, S. A. Teukolsky, W. T. Vetterling, and B. P. Flannery, *Numerical Recipes in C* (Cambridge University Press, Cambridge, 1992).